I&EC research
Industrial & Engineering Chemistry Research

Article

pubs.acs.org/IECR

Simulation and Control of Porosity in a Three-Dimensional Thin-Film Solar Cell

Jianqiao Huang,[†] Gerassimos Orkoulas,*[,†] and Panagiotis D. Christofides[†,‡]

[†]Department of Chemical and Biomolecular Engineering, University of California at Los Angeles (UCLA), Los Angeles, California 90095-1592, United States

[‡]Department of Electrical Engineering, University of California at Los Angeles (UCLA), Los Angeles, California 90095-1594, United States

ABSTRACT: This work focuses on the simulation and control of a three-dimensional (3D) porous silicon thin-film deposition process that is used in the manufacture of thin-film solar cell systems. Initially, a solid-by-solid 3D kinetic Monte Carlo (kMC) model is introduced to simulate the porous silicon thin-film deposition process, and the simulation parameters are tuned to generate porous silicon films with porosity values that match available experimental data. A closed-form differential equation model then is introduced to predict the dynamics of the film porosity computed by the kMC model, and the parameters in this model are identified by appropriate fitting to open-loop kMC simulation results. Subsequently, a model predictive controller (MPC) is designed and implemented on the kMC model. Closed-loop simulation results demonstrate that the thin-film porosity can be regulated to desired values.

INTRODUCTION

Solar energy is currently one of the most promising alternative energy sources, and thin-film silicon solar cells are currently the most widely used solar cell systems. Presently, the main obstacles for a wide use of solar power are the relatively high costs and the limited conversion efficiency of the solar energy.[1] Optimizing the light trapping process is one of the major aspects to improve the solar cell conversion efficiency and is one of the central research aspects nowadays (see, for example, refs 2 and 3). It has been found in previous research studies that surface morphology, which includes surface roughness and slope, at each film interface strongly affects the light trapping process,[4−8] and the use of porous silicon (PS) film as an intermediate layer between the substrate and the thin silicon film can improve the substrate backside reflectance and prevent the material contamination.[9−12] Specifically, it has been shown that a single porous silicon layer could serve as a seeding layer and is necessary for a sufficient light reflection.[9,13,14] Moreover, at the same time, this porous silicon layer could be a guttering barrier preventing impurity diffusion from the low-cost substrate into the active silicon layer.[15] Research also indicates that porous silicon can reduce solar cell optical losses from 37% to 8% and increase a short-circuit current by 25% and open-circuit voltage by 20 mV.[15] Thus, it is very important to develop a systematic way to simulate and control this porous silicon layer deposition process and improve the solar cell conversion efficiency. Despite its importance, this problem has not attracted much attention.

In the context of modeling and control of thin-film microstructure, two mathematical modeling approaches have been developed and widely used: kinetic Monte Carlo (kMC) methods and stochastic differential equation models. kMC methods were initially introduced to simulate thin-film microscopic processes. The required thermodynamic and kinetic parameters can be obtained from experiments and molecular dynamics simulations.[16−19] Since kMC models are not available in closed form, they cannot be readily used for feedback control design and system-level analysis. On the other hand, differential equation models can be derived from the corresponding master equation of the microscopic process and/or identified from process data.[19] The closed form of the differential equation models enables their use as the basis for the design of feedback controllers which can regulate thin-film porosity. Solid-on-solid models have been frequently used to simulate thin-film deposition processes; however, in these models, no vacancies are allowed inside the film.

Motivated by the above, in this work, we focus on simulation and control of porosity (expressed in terms of the concept of site occupancy ratio (SOR)) in a three-dimensional (3D) porous thin-film deposition process. Initially, a thin-film deposition process is modeled using the kMC method on a 3D solid-by-solid cubic lattice, where vacancies and overhangs are allowed to develop inside the film, and thin porous silicon films with SOR values that match available experimental data are deposited with this model. This process includes both a deposition process, in which the particles deposit onto the film, and a migration process, in which surface particles on lattice migrate to other lattice sites. A first-order ordinary differential equation (ODE) model is then used to describe the dynamics of film SOR and predict the evolution of film SOR. A model predictive control algorithm is finally developed on the basis of the dynamic equation model to regulate film SOR at desired levels. Closed-loop simulation results demonstrate the effective-

Special Issue: Multiscale Structures and Systems in Process Engineering

Received: January 28, 2013
Revised: February 19, 2013
Accepted: February 19, 2013
Published: February 19, 2013

dx.doi.org/10.1021/ie4003359 | *Ind. Eng. Chem. Res.* 2013, 52, 11246−11252

ness of the proposed model predictive control algorithm in successfully regulating the film SOR to desired levels that optimize thin-film light trapping.

PRELIMINARIES

Solid-by-Solid Cubic Lattice Kinetic Monte Carlo Model for Thin-Film Deposition Process. The thin-film growth process is simulated using a solid-by-solid kMC model via a 3D cubic lattice. Two microscopic processes are included in the kMC model: a deposition process, in which particles are incorporated into the film from the gas phase, and a migration process, in which surface particles move to adjacent available sites.[16,18,20,21] The growth direction is normal to the lateral directions. The number of sites in the lateral directions are defined as the lattice sizes and are denoted by L_x and L_y.

A solid-on-solid lattice model, in which a new particle deposits right above an existing particle, is widely used to simulate thin-film deposition processes. However, in the solid-on-solid model, the deposited film is condensed and no vacancy is allowed inside the film. Thus, it is not possible to use this model to describe and regulate the film SOR (or porosity). Therefore, the solid-by-solid cubic lattice model, which includes both a deposition process and a migration process, is proposed. In this work, a 3D solid-by-solid cubic lattice is utilized, and the maximum number of neighbors for each site is four.

Deposition Process. In a solid-by-solid model deposition event, one site is randomly selected for a deposition event. If the height of the selected site is equal or higher than all its neighbors, then a new particle is deposited on top of the selected site and the height of the selected column is increased by one. If the height of the selected site is lower than its neighbor(s), a new particle is deposited to the height where it has at least two neighboring particles, unless the particle is in contact with the existing particles beneath it, as shown in Figure 1. The microscopic adsorption rate (W), which is expressed in

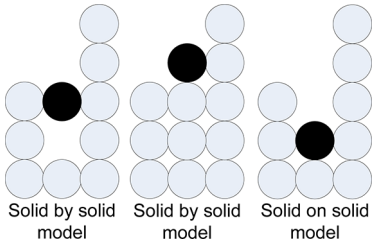

Figure 1. Differences between solid-on-solid model and solid-by-solid model in a deposition process.

units of layers per second, depends on the gas-phase concentration and is considered as a model input in this work. In this work, it is assumed that all incident particles have vertical incidence. For the entire deposition process, the microscopic adsorption rate (deposition rate) in terms of incident particles per unit time, which is denoted as r_a, is related to W as follows:

$$r_a = L_x \times L_y \times W \tag{1}$$

Migration Process. In this work, it is assumed that only surface particles with no neighbors are subject to migration process. Explicitly, in a solid-by-solid model migration event, the height of the selected migration site is always higher than all its neighbors, and the destination site is randomly selected among all its four neighboring sites. Figure 2 shows the major

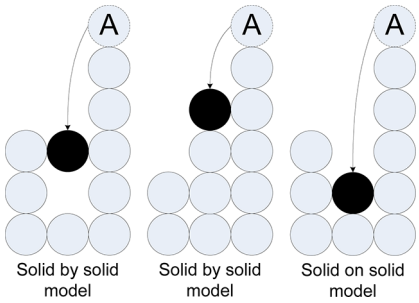

Figure 2. Differences between the solid-on-solid model and the solid-by-solid model in a migration process.

differences between a solid-on-solid model and a solid-by-solid model in a migration process. In the solid-on-solid model, once the particle (particle A) is selected to migrate to a target column, it deposits right above the existing particle of the target column and the height of the target column is increased by one particle, as is shown in the right part of Figure 2; in the solid-by-solid model, however, once the particle (particle A) is selected to migrate to a target column, it deposits to the height where it gets at least two neighboring particles, as is shown in the left part of Figure 2, unless this height is lower than the height of the target column in the corresponding solid-on-solid case, as is shown in the middle part of Figure 2. It is necessary to point out that Figures 1 and 2 depict a two-dimensional (2D) square lattice model to give a clear description of the model, but all the simulations in this work are carried out based on a 3D cubic lattice. The migration rate (probability) of a particle follows an Arrhenius-type law with a precalculated activation energy barrier that depends on the local environment of the particle, i.e., the number of the nearest neighbors of the particle chosen for a migration event. The migration rate of the ith particle is calculated as follows:

$$r_{m,i} = \nu_0 \exp\left(-\frac{E_s + n_i E_n}{k_B T}\right) \tag{2}$$

where ν_0 denotes the pre-exponential factor, n_i is the number of the nearest neighbors, and, in this work, $r_{m,i}$ is nonzero only if $n_i = 0$; E_s is the contribution to the activation energy barrier from the site itself, E_n is the contribution to the activation energy barrier from each nearest neighbor, k_B is the Boltzmann constant, and T is the substrate temperature of the thin film. Since the film is thin, the temperature is assumed to be uniform throughout the film and is treated as a time-varying but spatially invariant process parameter. The justification of the Arrhenius law dependence of the migration rate on temperature can be found in ref 22.

The solid-by-solid model is a more realistic representation than the original solid-on-solid model for silicon films. It is known that the activation energy E_n for silicon ranges from 0.6 eV to 0.9 eV. Once a particle gets two neighboring particles, the migration rate (moving possibility) is decreased by 10^6,[6,23] so it is extremely hard for any particles with more than two neighboring particles to further move downward.

Definition of Film Site Occupancy Ratio. Simulations of the kMC model of a 3D solid-by-solid porous silicon thin-film growth process are implemented utilizing the continuous-time Monte Carlo algorithm. To evaluate the thin-film microstructure (porosity) quantitatively, the film site occupancy ratio

dx.doi.org/10.1021/ie4003359 | Ind. Eng. Chem. Res. 2013, 52, 11246−11252

(SOR) is introduced in this subsection. The mathematical expression of film SOR is defined as follows:[24]

$$\rho = \frac{N}{L_x \times L_y \times H} \tag{3}$$

where ρ denotes the film SOR, N is the total number of deposited particles on the lattice, L_x and L_y are the lattice sizes on each direction, and H denotes the number of deposited layers. Since each layer contains $L_x \times L_y$ sites, the total number of sites in the film that can be contained within the H layers is $L_x \times L_y \times H$. Thus, film SOR is the ratio of the occupied lattice sites, N, over the total number of available sites, $L_x \times L_y \times H$. The film SOR value ranges from 0 to 1. Specifically, $\rho = 1$ denotes a fully occupied film with a flat surface. The value of zero is assigned to ρ at the beginning of the deposition process, since there are no particles deposited on the lattice.

Simulations are carried out to understand the dynamic behavior of SOR under different operating conditions. The time required to finish the simulation strongly depends on the operating conditions and the simulation time ranges from minutes to days. Figure 3 shows the SOR dynamic evolution

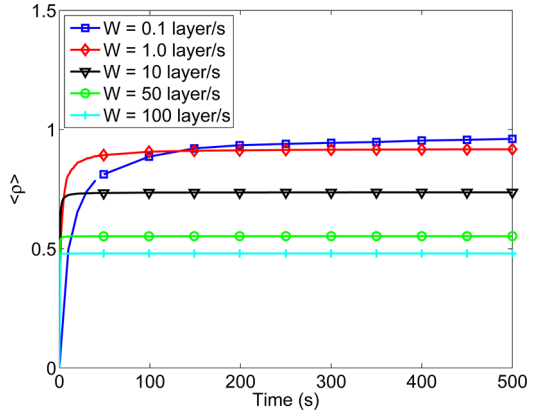

Figure 3. Time evolution profiles of the site occupancy ratio (SOR) values at different deposition rates.

plots at different deposition rates. It is clear that as the deposition rate increases, the film SOR decreases since increased deposition rates leave the particles less time and opportunities for migration. The SOR dynamics dependence on temperature is shown in Figure 4. As temperature increases,

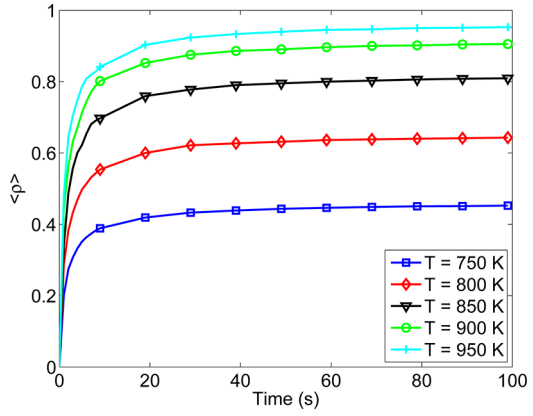

Figure 4. Time evolution profiles of SOR at different substrate temperatures.

the migration effect becomes stronger and the film particles migrate to increase the film SOR. Figure 5 shows the system

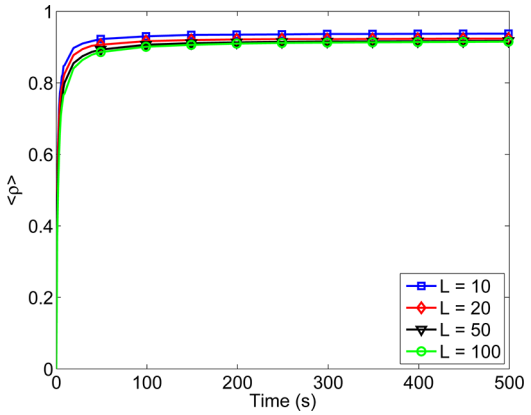

Figure 5. Time evolution profiles of SOR at different lattice sizes.

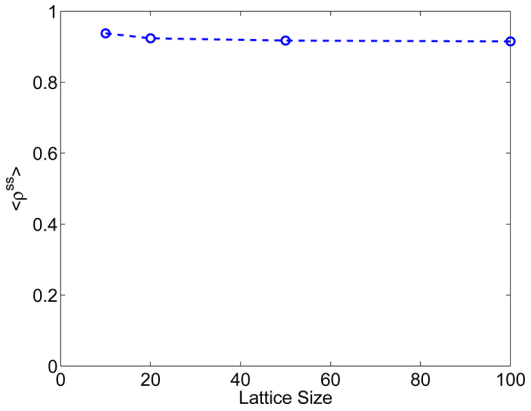

Figure 6. Film SOR steady-state values at different lattice sizes.

dynamics at different lattice sizes, and Figure 6 shows the SOR steady-state values dependence over lattice sizes (the SOR steady-state values are approximated by averaging the last 50 values of SOR evolution profiles). It is clear in this plot that lattice size has very limited influence over the system SOR dynamics; therefore, in this work, using a small lattice size ($L_x = L_y = 50$) to carry out the simulations will not affect the results or the conclusions.

DYNAMIC MODEL CONSTRUCTION AND PARAMETER ESTIMATION

Dynamic Model of Film Site Occupancy Ratio. Film porosity is characterized by the site occupancy ratio (SOR). According to the definition of film SOR given in eq 3, film SOR is a cumulative property, which accounts for all deposited layers during the entire deposition process, so its evolution can be characterized by an integral form. Before further derivation of the dynamic model of film SOR, the concept of instantaneous film SOR of the film layers deposited between time t and $t + \Delta t$, denoted by ρ_d, is first introduced as the spatial derivative of the number of deposited particles in the growing direction as follows:

dx.doi.org/10.1021/ie4003359 | Ind. Eng. Chem. Res. 2013, 52, 11246−11252

$$\rho_d = \frac{dN}{d(HL_xL_y)} \tag{4}$$

In eq 4, the lattice sizes L_x and L_y are constants and the derivative dH can be written as a linear function of time derivative dt as follows:

$$dH = r_H\, dt \tag{5}$$

where r_H is the growth rate of the thin film from the top layer point of view. The expressions of N and H can be obtained by integrating eqs 4 and 5 as follows:

$$N(t) = L\int_0^t \rho_d r_H\, ds$$
$$H(t) = \int_0^t r_H\, ds \tag{6}$$

With the definition of ρ of eq 3 and the expressions of N and H of eq 6, the film SOR of eq 3 can be rewritten in an integral form as follows:

$$\rho = \frac{\int_0^t \rho_d r_H\, ds}{\int_0^t r_H\, ds} \tag{7}$$

To simplify the subsequent development and develop an SOR model that is suitable for control purposes, we assume that the dynamics of the instantaneous film SOR (ρ_d) can be approximated by a first-order process, i.e.,

$$\tau\frac{d\rho_d(t)}{dt} = \rho_d^{ss} - \rho_d(t) \tag{8}$$

where τ is the time constant and ρ_d^{ss} is the steady-state value of the instantaneous film SOR. We note that the first-order ODE model of eq 8 was introduced and justified with numerical results in ref 24 for the modeling of the partial film SOR, which is defined to characterize the evolution of the film porosity of layers that are close to the film surface. In this sense, the instantaneous film SOR is a similar concept to the partial film SOR, because it also describes the contribution to the bulk film porosity of the newly deposited layers. Therefore, the first-order ODE model is a suitable choice to describe the evolution of the instantaneous film SOR.

From eq 7, it follows that, at large times, as ρ_d approaches ρ_d^{ss}, the steady-state film SOR (ρ^{ss}) approaches the steady-state value of the instantaneous film SOR (i.e., $\rho^{ss} = \rho_d^{ss}$). The deterministic ODE system of eq 8 is subject to the following initial condition:

$$\rho_d(t_0) = \rho_{d0} \tag{9}$$

where t_0 is the initial time and ρ_{d0} is the initial value of the instantaneous film SOR. From eqs 8 and 9, and the fact that $\rho^{ss} = \rho_d^{ss}$ at large times, it follows that

$$\rho_d(t) = \rho^{ss} + (\rho_{d0} - \rho^{ss})\, e^{-(t-t_0)/\tau} \tag{10}$$

For controller implementation purposes, the expression of the film SOR can be derived as follows:

$$\rho(t) = \frac{\int_0^{t_0}\rho_d r_H\, ds + \int_{t_0}^t \rho_d r_H\, ds}{\int_0^{t_0} r_H\, ds + \int_{t_0}^t r_H\, ds} = \frac{\rho(t_0)H(t_0) + \int_{t_0}^t \rho_d r_H\, ds}{H(t_0) + \int_{t_0}^t r_H\, ds} \tag{11}$$

where t_0 is the current time, $\rho(t_0)$ and $H(t_0)$ are the film SOR and the film height at time t_0, respectively.

Substituting the solution of ρ_d of eq 10 into eq 11 and assuming that r_H is constant for $t > \tau > t_0$, which is taken to be the case in the parameter estimation and the MPC formulations below, the analytical solution of film SOR at time t can be obtained as follows:

$$\rho = \rho(t_0)H(t_0) + r_H\left\{\rho^{ss}(t - t_0) + (\rho^{ss} - \rho(t_0))\tau \times \left[e^{-(t-t_0)/\tau} - 1\right]\right\}/[H(t_0) + r_H(t - t_0)] \tag{12}$$

which is directly utilized in the model predictive control formulation of eq 13 below.

Parameter Estimation. In the dynamic model of eq 8, two model parameters must be obtained from kMC data of the deposition process. These model parameters can be estimated by fitting the open-loop simulation data at fixed deposition rates from the kMC model to closed-form models by using least-squares methods.[24] In the parameter estimation, the predicted evolution profiles from the dynamic model of eq 8 and the ones from the kMC simulation of the deposition process are compared in a least-squares sense to determine the best model parameters.

Operating conditions, such as temperature and deposition rates, strongly affect the process dynamics and solar thin-film properties. Thus, the model parameters are functions of the operating conditions. In this work, we choose the deposition rate (W) as the manipulated input and keep the substrate temperature fixed at T = 900 K. Figure 7 shows the closed-form differential equation dynamics fitted to open-loop kMC simulations. It is clear that the closed-form model can accurately predict the SOR profile obtained from the kMC simulation. The dependence of the model parameters on the deposition rate W can be obtained by performing the parameter

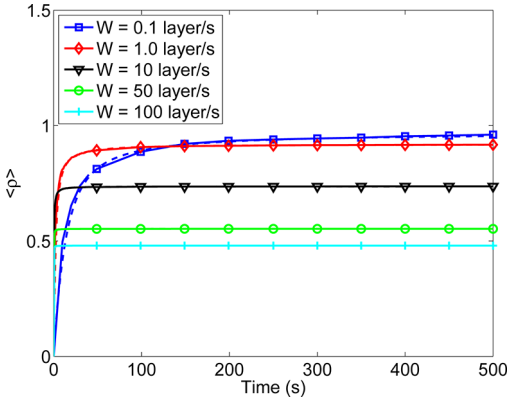

Figure 7. Closed-form model fitted to open-loop kMC simulation results.

dx.doi.org/10.1021/ie4003359 | Ind. Eng. Chem. Res. 2013, 52, 11246−11252

estimation procedure discussed above for a variety of deposition rate values (ranging from 0.1 layer/s to 100 layer/s); see Figures 8 and 9 for the dependence of the model

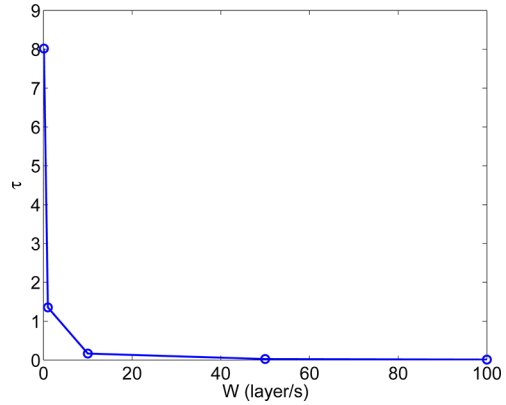

Figure 8. Dependence of τ on the deposition rate with a substrate temperature of T = 900 K.

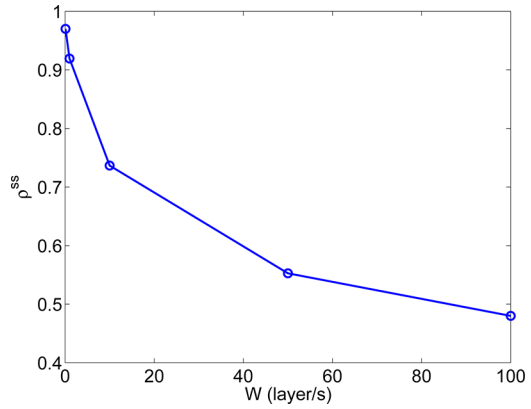

Figure 9. Dependence of ρ_{ss} on the deposition rate with a substrate temperature of T = 900 K.

parameters on the deposition rates. Simulation results from 100 independent simulation runs are used for the parameter estimation under each deposition rate condition. It can be clearly seen that the model parameters are strong functions of the deposition rate and this dependence is the basis for using W to control film porosity.

MODEL PREDICTIVE CONTROLLER DESIGN

In this section, a model predictive controller (MPC) is designed based on the dynamic model of film SOR to regulate the expected values of film SOR to desired levels by manipulating the deposition rate. The value of film SOR is assumed to be available to the controller. In practice, real-time estimates of film porosity can be obtained from a combination of in situ gas phase measurements and off-line thin-film porosity measurements. While it is difficult to obtain real-time direct measurements of film porosity, it is possible to use open-loop experimental data at different deposition conditions (including off-line porosity measurements) to construct a model that estimates film porosity from in-situ gas-phase measurements and combine this model with the model predictive control system proposed in this work; the reader may refer to ref 25 for an implementation of this approach in the context of thin-film carbon content measurement and control.

MPC Formulation. In this subsection, a model predictive control problem is formulated to regulate film SOR to desired values. The expected value of film SOR, $\langle\rho\rangle$, is chosen as the control objective. The deposition rate is used as the manipulated input. The substrate temperature is fixed at a certain value, T = 900 K, during all closed-loop simulations. It is necessary to point out that both the deposition rate and the temperature strongly influence the evolution of thin films and either or both can be used as manipulated variables. In the present case, we fix T = 900 K, because there are available experimental data in this temperature for porosity that allowed us to fine-tune our kMC model and, subsequently, the deposition rate became the natural choice for manipulated input, which allows us to reach a broad range of porosity values corresponding to experimental data. In addition, it should be noted that the proposed modeling and control methods do not depend on the specific number of the manipulated variables and can be easily extended to the case of multiple inputs. To account for several practical considerations, several constraints are added to the control problem. First, there is a constraint on the range of variation of the deposition rate. Another constraint is imposed on the rate of change of the deposition rate to account for actuator limitations. The control action at time t is obtained by solving an optimal control problem.

The cost function in the optimal control problem is defined as the deviation of $\langle\rho\rangle$ from its setpoint. The optimal profile of the deposition rate is calculated by solving an optimization problem in a receding horizon fashion. Specifically, the MPC problem is formulated as follows:

$$\min_{W_1,\ldots,W_i,\ldots,W_p} J = \sum_{i=1}^{p}\left[\frac{\rho_{\text{set}} - \rho(t_i)}{\rho_{\text{set}}}\right]^2 \tag{13}$$

subject to

$$\rho(t_i) = \rho(t_{i-1})\langle\bar{h}(t_{i-1})\rangle + r_h[\rho^{ss}\Delta + (\rho^{ss} - \rho(t_{i-1}))\tau \times (e^{-\Delta/\tau} - 1)]/(\langle\bar{h}(t_{i-1})\rangle + r_h\Delta)$$

$$W_{\min} < W_i < W_{\max}, \left|\frac{W_{i+1} - W_i}{\Delta}\right| \le L_W$$

$$i = 1, 2, \ldots, p$$

where t is the current time, Δ the sampling time, p the number of prediction steps, $p\Delta$ the specified prediction horizon, t_i the time of the ith prediction step ($t_i = t + i\Delta$, i = 1, 2, ..., p), W_i the deposition rate at the ith step ($W_i = W(t + i\Delta)$, i = 1, 2, ..., p), ρ_{set} the SOR setpoint, $W_{\min}$ the lower bound on the deposition rate, $W_{\max}$ the upper bound on the deposition rate, and L_W the limit on the rate of change of the deposition rate. These manipulated input constraints are added in the control system to address practical concerns such as capacity and response time of control actuators.

The dependence of the model parameters (ρ^{ss}) and τ on the deposition rate (W) of eq 13 is used in the formulation of the MPC. The parameters estimated under time-invariant operating conditions are suitable for the purpose of MPC design, because the control input in the MPC formulation is piecewise constant, i.e., the manipulated deposition rate remains constant between two consecutive sampling times, and thus, the dynamics of the

dx.doi.org/10.1021/ie4003359 | Ind. Eng. Chem. Res. 2013, 52, 11246−11252

microscopic process can be predicted using the dynamic models with the estimated parameters for the fixed value of W.

Regulation of Film Porosity by Manipulating the Deposition Rate. In this section, the proposed model predictive controller (MPC) of eq 13 is applied to the kMC model of the thin-film growth process described in the Preliminaries section. The value of the deposition rate is obtained from the solution of the problem of eq 13 at each sampling time and is applied to the closed-loop system until the next sampling time. The optimization problem in the MPC formulation of eq 13 is solved via a local constrained minimization algorithm, using a broad set of initial guesses.

The substrate temperature is fixed at 900 K and the initial deposition rate is 1.0 layer/s. The variation of deposition rate is from 0.1 layer/s to 100.0 layer/s. The maximum rate of change of the deposition rate is L_W = 10 layer/s^2. The time interval between two samplings is 1 s. The time it takes to solve an optimization problem at each sampling time is ∼1 s, which is comparable to the sampling time. The closed-loop simulation duration is 200 s. All expected values are obtained from 100 independent simulation runs.

The relationship between the film SOR and reflectance can be approximated using Figure 10.[1] The triangles in Figure 10

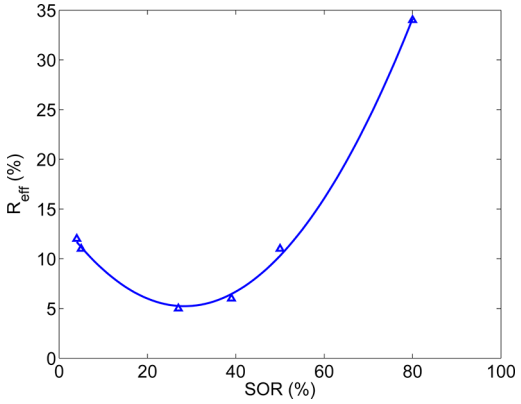

Figure 10. Relationship between the film SOR and reflectance.

are obtained from experiments, and the curve is the fitting result based on a quadratic function. Based on this plot, two different SOR setpoints—ρ = 0.5 and ρ = 0.8, which correspond to reflectance values, R = 0.35 and R = 0.1, respectively—are picked to demonstrate the designed closed-loop system. These setpoints are commonly desired for porous silicon SOR for improved light trapping performance.[9,15] Figures 11 and 12 show the evolution profiles of the expected film SOR from the closed-loop simulations of the porosity control problem and the corresponding input deposition rate profiles. The MPC successfully drives the expected film SORs to the set-point values. Finally, we note that while a finite-dimensional model is used to describe the dynamics of film porosity as a function of the deposition rate, the spatial distribution of the pores inside the film is taken into account in the kMC model and the entire film porosity is regulated at the desired values.

Dual Porosity Regulation with Model Predictive Controller. In the solar panel industry, it is very common to use dual-porosity silicon layers between the substrate and the thin silicon film.[9,26] Dual-porosity silicon layers are composed of two independent layers with different SOR values. In

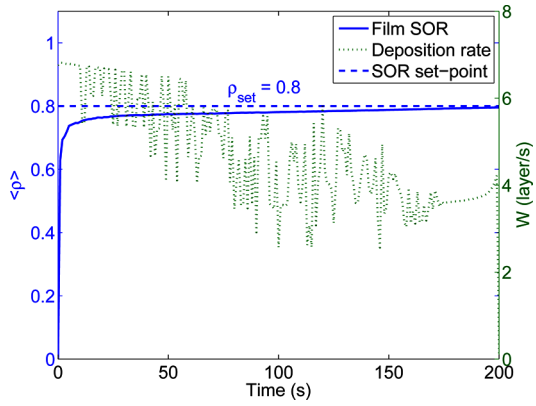

Figure 11. Profiles of film SOR (solid line) and of the deposition rate (dotted line) under closed-loop operation; SOR control with ρ_{set} = 0.8.

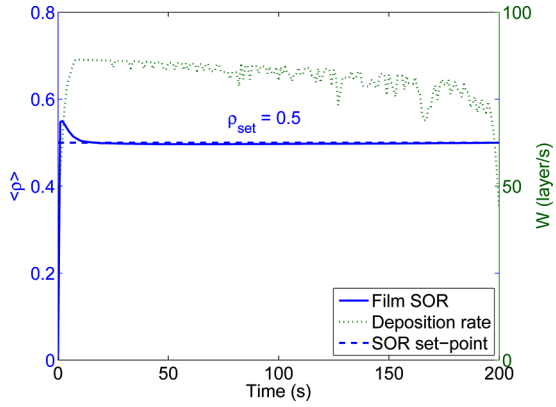

Figure 12. Profiles of film SOR (solid line) and of the deposition rate (dotted line) under closed-loop operation; SOR control with ρ_{set} = 0.5.

previous work, a two-stage dual-porosity control system was introduced to regulate two independent SOR values in a 2D film growth process simultaneously, and the same control system is applied to the 3D solid-by-solid model in this work. The details of the two-stage control system can be found in ref 27. Closed-loop simulations are carried out to demonstrate this two-stage dual porosity control framework. The simulation time for both periods is t_1 = t_2 = 200 s; set points for both stages are picked as $\rho_{set,1}$ = 0.8 and $\rho_{set,2}$ = 0.5. As is shown in Figure 13, the film SORs reach their setpoints accurately at the end of each stage.

CONCLUSIONS

A porous silicon thin-film deposition process, which is commonly used in the manufacture of thin-film solar cells, is considered in this work. The process is initially simulated via the kinetic Monte Carlo (kMC) method via a three-dimensional solid-by-solid model. A closed-form differential equation model then is introduced to predict the dynamics of film porosity, and the parameters in this model are identified by appropriate fitting to open-loop kMC simulation results. A model predictive controller (MPC) is designed and multiple setpoints are picked to demonstrate the controller performance, and the control system is extended to regulate the film SOR values of two independent film layers in a single deposition run.

dx.doi.org/10.1021/ie4003359 | Ind. Eng. Chem. Res. 2013, 52, 11246−11252

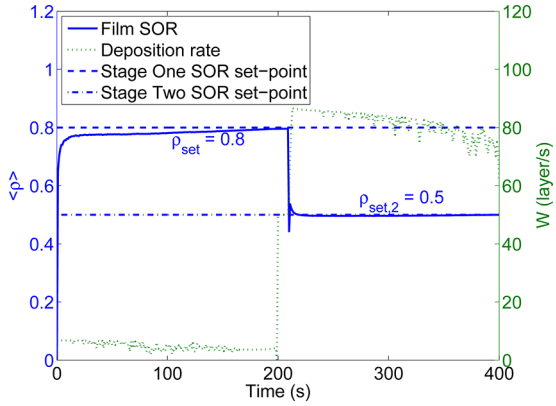

Figure 13. Profiles of film SOR (solid line) and of the deposition rate (dotted line) under two-stage dual-porosity closed-loop operation.

Results demonstrate that film SOR can be regulated to experimentally determined setpoints.

AUTHOR INFORMATION

Corresponding Author

*E-mail: makis@seas.ucla.edu.

Notes

The authors declare no competing financial interest.

ACKNOWLEDGMENTS

Financial support from the National Science Foundation (No. CBET-0652131) is gratefully acknowledged.

REFERENCES

(1) Yerokhov, V.; Melnyk, I. Porous silicon in solar cell structures: A review of achievements and modern directions of further use. *Renew. Sustainable Energy Rev.* **1999**, *3*, 291−322.

(2) Krč, J.; Smole, F.; Topič, M. Analysis of light scattering in amorphous Si:H solar cells by a one-dimensional semi-coherent optical model. *Progress Photovoltaics: Res. Appl.* **2003**, *11*, 15−26.

(3) Müller, J.; Rech, B.; Springer, J.; Vanecek, M. TCO and light trapping in silicon thin film solar cells. *Solar Energy* **2004**, *77*, 917−930.

(4) Zeman, M.; Vanswaaij, R. Optical modeling of a-Si:H solar cells with rough interfaces: Effect of back contact and interface roughness. *J. Appl. Phys.* **2000**, *88*, 6436−6443.

(5) Poruba, A.; Fejfar, A.; Remeš, Z.; Špringer, J.; Vaněček, M.; Kočka, J. Optical absorption and light scattering in microcrystalline silicon thin films and solar cells. *J. Appl. Phys.* **2000**, *88*, 148−160.

(6) Huang, J.; Orkoulas, G.; Christofides, P. D. Simulation and control of aggregate surface morphology in a two-stage thin film deposition process for improved light trapping. *Chem. Eng. Sci.* **2012**, *71*, 520−530.

(7) Huang, J.; Orkoulas, G.; Christofides, P. D. Modeling and control of transparent conducting oxide layer surface morphology for improved light trapping. *Chem. Eng. Sci.* **2012**, *74*, 135−147.

(8) Huang, J.; Orkoulas, G.; Christofides, P. D. Surface morphology control of transparent conducting oxide layers for improved light trapping using wafer grating and feedback control. *Chem. Eng. Sci.* **2012**, *81*, 191−201.

(9) Bilyalov, R.; Stalmans, L.; Beaucarne, G.; Loo, R.; Caymax, M.; Poortmans, J.; Nijs, J. Porous silicon as an intermediate layer for thin-film solar cell. *Sol. Energy Mater. Sol. Cells* **2001**, *65*, 477−485.

(10) Vitanov, P.; Kamenova, M.; Tyutyundzhiev, N.; Delibasheva, M.; Goranova, B.; Peneva, M. High-efficiency solar cell using a thin porous silicon layer. *Thin Solid Films* **1997**, *297*, 299−303.

(11) Yue, Z.; Shen, H.; Zhang, L.; Liu, B.; Gao, C.; Lv, H. Heterojunction solar cells produced by porous silicon layer transfer technology. *Appl. Phys. A: Mater. Sci. Process.* **2012**, *108*, 929−934.

(12) Dzhafarov, T.; Aslanov, S.; Ragimov, S.; Sadigov, M.; Yuksel, S. Effect of nanoporous silicon coating on silicon solar cell performance. *Vacuum* **2012**, *86*, 1875−1879.

(13) Krotkus, A.; Grigorasa, K.; Pačebutasa, V.; Barsonyb, I.; Vazsonyib, B.; Friedb, M.; Szlufcikc, J.; Nijsc, J.; Levy-Clement, C. Efficiency improvement by porous silicon coating of multicrystalline solar cells. *Sol. Energy Mater. Sol. Cells* **1997**, *45*, 267−273.

(14) Najar, A.; Charrier, J.; Pirasteh, P.; Sougrat, R. Ultra-low reflection porous silicon nanowires for solar cell applications. *Opt. Express* **2012**, *20*, 16861−16870.

(15) Bilyalov, R.; Stalmans, L.; Schirone, L.; Levy-Clement, C. Use of porous silicon antireflection coating in multicrystalline silicon solar cell processing. *IEEE Trans. Electron Devices* **1999**, *46*, 2035−2040.

(16) Levine, S. W.; Engstrom, J. R.; Clancy, P. A kinetic Monte Carlo study of the growth of Si on Si(100) at varying angles of incident deposition. *Surf. Sci.* **1998**, *401*, 112−123.

(17) Zhang, P.; Zheng, X.; Wu, S.; Liu, J.; He, D. Kinetic Monte Carlo simulation of Cu thin film growth. *Vacuum* **2004**, *72*, 405−410.

(18) Levine, S. W.; Clancy, P. A simple model for the growth of polycrystalline Si using the kinetic Monte Carlo simulation. *Modell. Simul. Mater. Sci. Eng.* **2000**, *8*, 751−762.

(19) Christofides, P. D.; Armaou, A.; Lou, Y.; Varshney, A. *Control and Optimization of Multiscale Process Systems*; Birkhäuser: Boston, 2008.

(20) Wang, L.; Clancy, P. Kinetic Monte Carlo simulation of the growth of polycrystalline Cu films. *Surf. Sci.* **2001**, *473*, 25−38.

(21) Yang, Y. G.; Johnson, R. A.; Wadley, H. N. A Monte Carlo simulation of the physical vapor deposition of nickel. *Acta Mater.* **1997**, *45*, 1455−1468.

(22) Binder, K.; Kalos, M. H. Critical clusters" in a supersaturated vapor: Theory and Monte Carlo simulation. *J. Stat. Phys.* **1980**, *22*, 363−396.

(23) Keršulis, S.; Mitin, V. Monte Carlo simulation of growth and recovery of silicon. *Mater. Sci. Eng. B* **1995**, *29*, 34−37.

(24) Hu, G.; Orkoulas, G.; Christofides, P. D. Modeling and control of film porosity in thin film deposition. *Chem. Eng. Sci.* **2009**, *64*, 3668−3682.

(25) Ni, D.; Lou, Y.; Christofides, P. D.; Sha, L.; Lao, S.; Chang, J. P. Real-time carbon content control for PECVD ZrO_2 thin-film growth. *IEEE Trans. Semicond. Manuf.* **2004**, *17*, 221−230.

(26) Jin, S.; Bender, H.; Stalmans, L.; Bilyalov, R.; Poortmans, J.; Loo, R.; Caymax, M. Transmission electron microscopy investigation of the crystallographic quality of silicon films grown epitaxially on porous silicon. *J. Cryst. Growth* **2000**, *212*, 119−127.

(27) Huang, J.; Orkoulas, G.; Christofides, P. D. Porosity Control in Thin Film Solar Cells. *Chem. Eng. Sci.*, in press.